JOURNAL OF Materials CHEMISTRY

Photocontrol of liquid motion on an azobenzene monolayer

Sang-Keun Oh,† Masaru Nakagawa and Kunihiro Ichimura*‡

Chemical Resources Laboratory, Tokyo Institute of Technology, 4259 Nagatsuta, Midori-ku, Yokohama 226-8503, Japan

Received 26th November 2001, Accepted 17th May 2002
First published as an Advance Article on the web 27th June 2002

This paper describes a novel strategy for the non-mechanical motion of a liquid droplet by photoisomerization of surface-immobilized azobenzenes. When a liquid droplet is placed on a substrate surface that has been modified with a monolayer of azobenzene-terminated calix[4]resorcinarenes, alternating irradiation with UV and blue light causes *in situ* changes in the contact angle of the droplet. The spreading/retraction motion of a liquid droplet is based on the reversible change in surface free energy of the photoresponsive surface due to the *trans–cis* isomerization of the azobenzene molecules. By measuring the hysteresis in contact angles of various liquids, we determined the principal requirement for the motion of a liquid droplet to occur: a receding contact angle on a *trans*-rich surface should be larger than an advancing contact angle on a *cis*-rich surface. Localized illumination of a liquid droplet of several millimeters in diameter causes it to move vectorially across the photoresponsive surface. The direction and velocity of the motion are tailored by manipulating both the direction and steepness of an applied light intensity gradient. Detailed profiles of a moving droplet support the assumption that the surface-assisted motion is ascribed to an imbalance in contact angles. The potential applicability of light-driven motion to lab-on-a-chip technology was presented by delivery of reactants for a chemical reaction on a photoresponsive surface by illumination.

Introduction

Interest in microfluidic devices has increased dramatically in the light of their high performance in biological and chemical analyses and combinatorial chemical synthesis.[1–6] For their operation, microfluidic devices must contain a number of miniaturized elements for pretreatment, reaction, separation and detection depending on the application. In addition, these elements need some means to position bulk fluid through microchannels. An efficient method useful for microscale devices involves non-mechanical electroosmotic flow.[7–9] The technology has rapidly expanded because of several advantages over pressure-driven flow using mechanical pumps, including (i) the technology is amenable to miniaturization and (ii) no moving parts are needed because the pumping of fluids is achieved simply by applying electric fields along the microchannels.[10] However, because a microfluidic system consists of many elements, the high voltages used for electroosmotic pumping may limit the ability to integrate sensitive electronic components in the same device.[4] In this paper we describe an alternative approach to the development of non-mechanical methods for liquid motion that is driven entirely by light. The method is based on the reversible photoisomerization of surface-immobilized azobenzenes.

When a liquid droplet is placed in contact with a solid surface, capillary forces drive the interface toward an equilibrium.[11] In the case of partial wetting, the droplet spreads symmetrically to give an equilibrium contact angle of $\theta > 0^\circ$. The dynamics of the spontaneous spreading are usually described at the macroscopic level by an energy balance between the capillary driving force and the hydrodynamic resistance to spreading.[12–15] On the other hand, if a liquid droplet is put in contact with a substrate with a spatial inhomogeneity in surface tension, an imbalance in the capillary forces is generated at the edges of the droplet.[16] This force imbalance causes the droplet to move so as to compensate the imbalanced force. The experimental observation of such a liquid motion has been reported by Chaudhury and Whitesides.[17] They demonstrated a water droplet running uphill by using a silanized silica surface with a hydrophobicity gradient. Liquid motion based on either temperature or concentration gradients has also been observed.[18–20] This type of liquid motion is referred to as Marangoni flow.[21] A classical example of liquid motion is the well-known "tears of wine", which results from the local increase in surface tension in wine caused by the evaporation of alcohol. Another example of the Marangoni flow is preferential solubilization of volatile components into one side of a liquid droplet, which causes motion of the droplet.[22,23] Electrochemically induced-gradients in surface tension maintained by the generation of surface-active species at one electrode and the consumption of them at another electrode have also been used to drive fluid motion.[24,25] Recently, the movement of liquids caused by non-covalent adsorption of alkylamines on a CO_2H-terminated surface was reported by Lee and Laibinis.[26]

Because the surface free energies of flat solid substrates are determined by the constitution at the atomic level of their outermost surfaces,[27] the alteration of the chemical structures of the outermost monomolecular layers by light (or some other external stimulus) can be used to trigger and manipulate various interfacial phenomena including wettability,[28,29] liquid crystal alignment,[30] dispersibility[31] and biomaterial affinity.[32] Thus, if a gradient in surface energy is generated photochemically as a result of spatially controlled changes of chemical structures at the outermost surface of a solid substrate, the motion of a liquid can be guided by spatially controlled photoirradiation of the photoresponsive substrate surface on which the liquid is placed. A solid surface modified with photochromic azobenzenes is a promising material to control surface free energy with light, because *trans–cis* photoisomerization of azobenzenes is accompanied by reversible changes

†*Present address*: Department of Chemistry, Texas A&M University, College Station, Texas, TX 77842-3012, USA.
‡*Present address*: Research Institute for Science and Technology, Tokyo University of Science, 2641 Yamazaki, Noda, Chiba 2780-8510, Japan. E-mail: ichimura@rs.noda.sut.ac.jp; Fax: +81-471-23-7814; Tel: +81-471-24-1501 (Ext. 5042).

 DOI: 10.1039/b110825p

This journal is © The Royal Society of Chemistry 2002

in the physicochemical properties of the chromophores such as dipole moment and geometrical molecular structure.[33]

This paper describes the light-driven motion of a liquid droplet on a chemisorbed azobenzene monolayer, thereby providing new principles for the design and operation of microfluidic devices. In this study, we use an *O*-octacarboxymethylated calix[4]resorcinarene (H-CRA-CM) with pendent *p*-octylazobenzene units as a photoresponsive adsorbate. The motion of liquid droplets was examined by placing them on the photoresponsive surface, and then photoirradiating them with UV and blue light to trigger the isomerization of the azobenzene moieties assembled on the surface. In a previous communication we described the vectorial motion across an H-CRA-CM-modified surface caused by spatially controlled illumination.[34]

Experimental

Materials

H-CRA-CM was synthesized through the Williamson coupling of 2,8,14,20-tetrakis(3-iodopropyl)-4,6,10,12,16,18,22,24-octakis(ethoxycarbonylmethoxy)calix[4]arene with the corresponding 4-phenylazophenol according to our previous report.[35] All organic reagents used as probe liquids for contact angle measurements were obtained from commercial sources. Diiodomethane, 1-bromonaphthalene and 1-methylnaphthalene were passed through an equal volume of alumina prior to use. Water was used after deionization and filtration through a Millipore Q system. Nematic liquid crystals (LCs) of NPC-02 (T_{NI} = 35.0 °C), a binary mixture of alkoxyphenylcyclohexane derivatives, and 5CB (T_{NI} = 35.4 °C), 4-cyano-4′-pentylbiphenyl, were donated by Rodic Co., Ltd. Fluorescamine and dodecylamine were obtained from Aldrich.

Monolayer preparation

A fused silica substrate (10 × 30 × 1 mm) was ultrasonically cleaned in a solution of piranha (**CAUTION**: piranha solution should be handled with great care; it has detonated unexpectedly) for 1 h, washed with copious amounts of deionized water and subsequently with acetone, and dried under vacuum. After cleaning, the substrate was immersed immediately in a solution of freshly distilled (3-aminopropyl)diethoxymethylsilane (0.25 g) in dry toluene (25 g) for 1 h at 25 °C. The substrate was washed with dry toluene, baked for 30 min at 120 °C, sonicated in toluene and methanol for 2 min each and finally dried in a vacuum. The silanized substrate was then immersed in a 1×10^{-4} mol dm^{-3} THF solution of H-CRA-CM for 30 min at 40 °C. A chemisorbed H-CRA-CM monolayer tethered to the aminated silica substrate was obtained after rinsing thoroughly with THF and then dried for 30 min at 80 °C.

Photoirradiation

Light sources of UV light (365 nm) and visible light (436 nm) were obtained from a 200 W Hg–Xe lamp (San-ei Electric, Supercure-203S) using suitable combinations of Toshiba glass filters, UV-35 + UV-D36A and Y-43 + V-44 for 365 nm and 436 nm light, respectively. Light intensity was measured with an optical power meter (Advantest TQ8210).

Physical measurements

UV-vis spectra of monolayers were recorded on a weak absorption spectrophotometer (JASCO, MAC-1). Advancing and receding contact angles were measured with a contact angle meter (Kyowa Interface Science, SA-11) in air at 23 °C. Advancing contact angles were taken as the maximum contact angle observed during the enlargement of a drop size. Receding contact angles were measured by reducing the size of the drops. Each contact angle reported here represents an average of 5–10 measurements made on different areas of a sample surface with errors of ± 2°. Contact angles for the *cis*-state correspond to those of the surface azobenzenes in a photostationary state after UV light irradiation. To evaluate the temperature dependence of the wetting properties of liquids (NPC-02 and 1-bromonaphthalene) on H-CRA-CM monolayers, sessile contact angles on H-CRA-CM-modified substrates were measured by placing them on a copper plate equipped with a heating circulator. Temperatures of the plate were calibrated with a digital surface thermometer. Thus temperatures described here indicate interface temperatures between a liquid droplet and the H-CRA-CM substrate. Drops placed on the substrates were equilibrated for 1 min at each temperature before reading contact angles. The reproducibility of readings was ± 1°.

Results and discussion

H-CRA-CM monolayers as a photoresponsive surface

The photoresponsive monolayers of H-CRA-CMs with four *p*-octylazobenzene residues were prepared simply by immersing aminosilylated silica plates in a dilute solution of H-CRA-CM. The resulting monolayer exhibited high desorption-resistance even toward polar solvents, such as water, because of the electrostatic interactions between the CO_2H groups of the H-CRA-CMs and the aminosilanized surface.[36] As discussed in our previous papers,[37] H-CRA-CM was designed to ensure sufficient free volume for *trans–cis* photoisomerization of the azobenzene moieties, even if the cyclic skeletons of H-CRA-CM are closely packed. This is because the molecular packing in this kind of SAM is determined specifically by the base area of the rigid cylindrical macrocycle. Consequently, a free volume exists in the kind of monomolecular film in which azobenzene residues are attached to the lower rim of the cyclic skeletons, thus leading to efficient *trans–cis* photoisomerizability.

We first confirmed that the photoirradiation of an H-CRA-CM monolayer with UV (365 nm) light results in the formation of the *cis*-isomer from the UV-vis spectra. Fig. 1(a) shows that the level of *trans–cis* photoisomerization is as large as ~90% even in a closely packed monolayer. The existence of isosbestic points in the spectra leads us to conclude

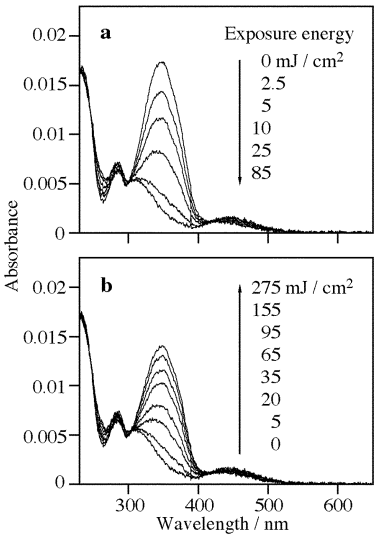

Fig. 1 UV-vis spectral changes of H-CRA-CM absorbed on a monolayer upon irradiation with 365 nm light (a) and with 436 nm light (b).

that only two species (*trans* and *cis* isomers) are involved in the photoreaction without any concomitant side reaction. Because the isomerization of azobenzene molecules is always accompanied by certain changes in dipole moment as well as geometrical shape,[33] the outermost surface of a UV-exposed H-CRA-CM monolayer is likely terminated by *cis*-azobenzenes with a higher dipole moment, leading to an increase in surface free energy.[28] Experimental results obtained by Zisman plots[11,38] revealed that the critical surface tension of the UV-exposed monolayer is 3.5 mJ m^{-2} higher than that of the monolayer before illumination. Photoirradiation of the *cis*-rich surface with blue (436 nm) light causes the *cis*-isomer to reverse into the *trans*-isomer (Fig. 1(b)).

In situ spreading/retraction motion of liquid droplets

Experiments investigating the light-driven motion of liquids were performed using chemisorbed monolayers of H-CRA-CM. Fig. 2 shows the *in situ* and reversible spreading/retraction motion of a droplet of the liquid crystal NPC-02 on substrates modified with H-CRA-CMs upon alternating irradiation with homogeneous UV and blue light. Illumination of the *trans*-rich surface with UV light led to a lateral spreading of the droplet on the surface because of the generation of the *cis*-isomers as discussed above. The sessile contact angle of the droplet was changed from 24° to 11° after UV irradiation. The droplet could be subsequently retracted by illumination with blue light, and all the changes were completely reversible. The durability of the photoresponsive surface was investigated by monitoring the *in situ* expanding/retraction motion of an NPC-02 droplet upon alternating irradiation with UV and blue light. Reversible changes of sessile contact angles (24° on *trans*-surface and 11° on *cis*-surface) were maintained within experimental error even after 100 cycles of alternating photoirradiation.

Surface-induced motion was also viable for the other nematic liquid crystals including 5CB and even for olive oil, 1-methylnaphthalene and 1,1,2,2-tetrachloroethane. However, some liquid droplets such as water, formamide and ethylene glycol could not be moved using the same illumination. This result is not surprising and can be attributed to the dynamic properties of the liquid/solid interfaces. Changes in equilibrium thermodynamic properties upon illumination provide an essential driving force for motion to occur. Liquid motion on a solid substrate, however, is primarily governed by dynamic factors such as the hysteresis of contact angles.[39] Hysteresis is a common occurrence for almost all types of practical interfacial phenomena and arises from molecular rearrangements occurring at the solid/liquid interfaces after they have come into contact with each other.[40–42] To address the effect of hysteresis on the light-guided movement of droplets, contact angle hysteresis, defined as the difference between advancing (θ_{adv}) and receding (θ_{rec}) contact angles, for these liquids on H-CRA-CM-modified substrates was measured before and after UV light irradiation (Table 1). As expected, liquids that show no *in situ* motion exhibited large contact angle hystereses.

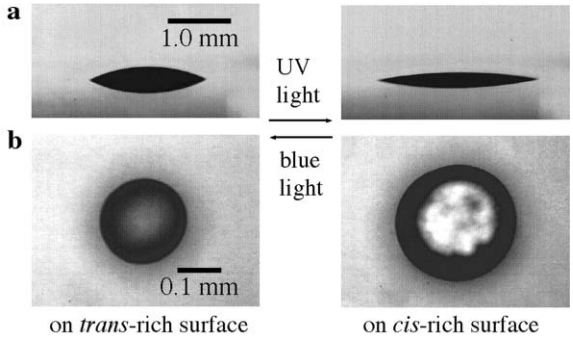

Fig. 2 Lateral (a) and top (b) views of *in situ* spreading/retraction motion of NPC-02 droplets on H-CRA-CM-modified plates upon homogeneous irradiation with UV and blue light. The sessile contact angles before and after UV irradiation were 24° and 11°, respectively.

In contrast, liquids displaying *in situ* and reversible changes in contact angles exhibited hystereses that were smaller than the extent of the light-induced changes in contact angles. Based on these results, we conclude that the motion of a droplet can be caused by light if the liquid droplet fulfills the following condition: θ_{rec} for the *trans*-isomer (θ^{tr}_{rec}) must be larger than θ_{adv} for the *cis*-isomer (θ^{cis}_{adv}). Because this condition includes both equilibrium thermodynamic and dynamic factors, it should be applicable to other approaches to move liquids due to driving forces arising from changes in the contact angle.[17] Note that NPC-02, relative to common organic liquids, exhibits both smaller hysteresis and larger photoinduced changes in contact angles upon photoisomerization (Table 1), hence it is quite suitable for quantitative interpretation of light-driven motion.

Displacement of liquid droplets

Because a gradient in surface tension induces a net mass transport of liquids,[16] we hypothesized that spatially controlled photoirradiation of a liquid droplet on H-CRA-CM-modified substrates could give the droplet directional motion. Fig. 3 shows the directional motion of an olive oil droplet on a *cis*-rich surface upon asymmetrical illumination with blue light. Olive oil is a liquid that fulfills the necessary condition to move (Table 1). Light with asymmetrical intensity was easily obtained from the edge of a focused light beam. Fig. 4 shows a typical intensity gradient of a light beam from a Xe–Hg lamp. For continuous motion we used gradient of blue light of region A in Fig. 4 . The gradient in light intensity between the advancing and receding edges of the moving droplet was constantly maintained by moving the light beam, which continued to move the droplet. Therefore, our photochemical method has no theoretical limitation on the distance that a droplet can be moved. To stop the movement of the droplet, the photoresponsive surface was irradiated with a homogeneous blue light (Fig. 3(c)).

The direction of movement of the droplet was controlled by varying the direction of the light intensity gradient (Fig. 3(d)). The velocity of the droplet intrinsically relies on both the steepness and intensity of the light gradient. A typical speed of 35 μm s^{-1} was observed for the motion of a ~2 μl droplet of olive oil. When a droplet on a *trans*-rich surface was subjected to asymmetrical irradiation with UV light having a less steep gradient in light intensity (Fig. 4, region B), the droplet displayed asymmetrical spreading rather than continuous movement. This type of spreading behavior can be used to cause the stepwise motion of a liquid droplet upon alternating

Table 1 Contact angles (°) of H-CRA-CM monolayer for various liquids[a]

	trans-Rich		*cis*-Rich	
	θ_{adv}	θ_{rec}	θ_{adv}	θ_{rec}
No motion				
Water	94	40	86	51
Formamide	68	17	62	19
Ethylene glycol	61	36	56	39
Poly(ethylene glycol)[b]	42	37	38	31
Motion				
1-Methylnaphthalene	26	24	20	18
1,1,2,2-Tetrachloroethane	18	16	12	11
5CB	43	37	22	19
NPC-02	28	24	11	10
Olive oil	29	25	17	13

[a]The values were within an experimental error of ± 2°. [b]Average molecular weight was 400.

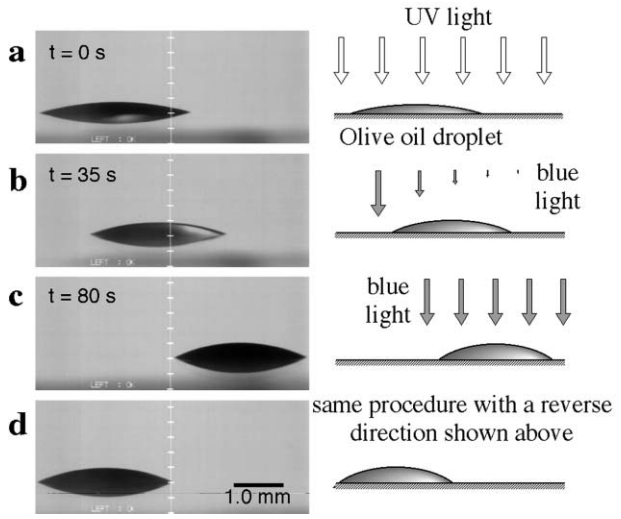

Fig. 3 Lateral photographs of light-driven motion of an olive oil droplet on a silica substrate modified with H-CRA-CM. The olive oil droplet on a *cis*-rich surface moved in a direction of higher surface energy by asymmetrical irradiation with 436 nm light perpendicular to the surface. (a, b and c) The sessile contact angles were changed from 18° to 25°. (d) The direction of movement of the droplet was controllable by varying the direction of the photoirradiation.

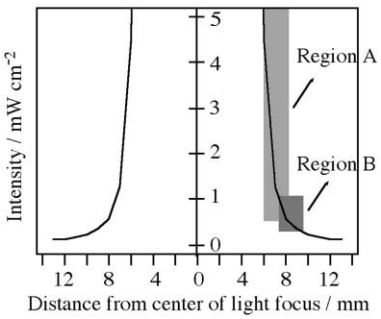

Fig. 4 A typical intensity gradient of a focused light beam from a Hg–Xe lamp. Irradiation of H-CRA-CM monolayers with light of region A causes continuous motion, while stepwise motion is induced by irradiation with light of region B .

irradiation with UV and blue light as demonstrated in Fig. 5. The force caused by the capillary imbalance due to the asymmetrical spreading is also sufficient to transport even a solid particle of mm scale. Fig. 6 shows the light-driven displacement of a glass bead by the action of the alternating spreading and dewetting of an NPC-02 droplet. Because the asymmetrical spreading and dewetting of NPC-02 causes deformation of the equilibrium meniscus between the liquid and the glass bead, a spatial inhomogeneity in the capillary force occurs in the coalesced liquid. This imbalanced capillary force is responsible for displacement of the glass bead. The usefulness of the photochemical method reported here is supported by the motion of liquid set in a glass tube. Fig. 7 shows the movement of NPC-02 placed in a glass tube, the inside wall of which was modified with the H-CRA-CM in advance. When light irradiation is carried out in the manner shown in Fig. 3, fluid motion in the glass tube can be controlled on demand.

Mechanism of light-driven motion of liquids

This section presents a brief description of the kinetics of the *in situ* spreading of a liquid droplet and the driving mechanism of its directional motion.

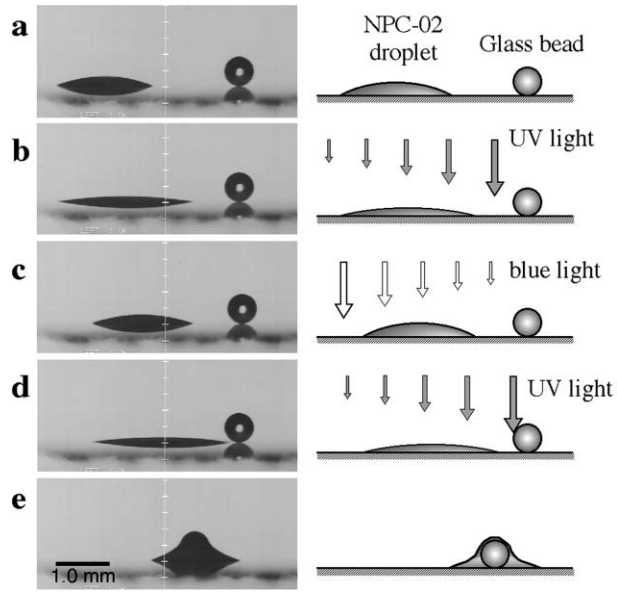

Fig. 5 Light-driven motion of an NPC-02 droplet on a H-CRA-CM-modified plate to capture a glass bead (diameter ~0.5 mm). A droplet was placed on a H-CRA-CM-modified plate (a), followed by UV light irradiation at the right edge of the droplet to cause an asymmetrical spreading (b). Subsequent irradiation with blue light at the left edge resulted in dewetting, leading to the displacement of the droplet (c). The repetition of this stepwise photoirradiation resulted in the approach of the droplet to the bead, which was finally captured by the liquid (e).

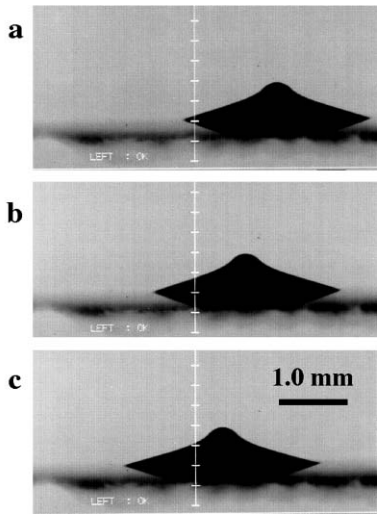

Fig. 6 Light-driven motion of a glass bead by the action of the alternating spreading and dewetting of an NPC-02 droplet on a H-CRA-CM-modified plate. Photoirradiation of the plate was carried out by the same procedure as shown in Fig. 5. Each photograph is a result of 4-cycles of the alternating spreading and dewetting processes of the preceding frame and shows the droplet on a *trans*-rich surface.

When a small liquid droplet is put in contact with a flat solid surface, the liquid droplet has a finite contact angle in a partial wetting situation.[43] If the radius of the drop is smaller than the Laplace length, gravity effects are negligible and the droplet forms a spherical cap. At equilibrium, the corresponding contact angle θ_e is given by the Young relation.[11] This equation expresses the balance of horizontal forces. If a liquid droplet is placed on a photoresponsive H-CRA-CM monolayer, illumination of the surface instantly alters the surface energy as discussed above. In this situation the contact angle θ differs from its equilibrium value θ_e This leads to an imbalance in the horizontal capillary forces, so that there is a total pulling force, F_h, responsible for the spreading (or retraction) of the

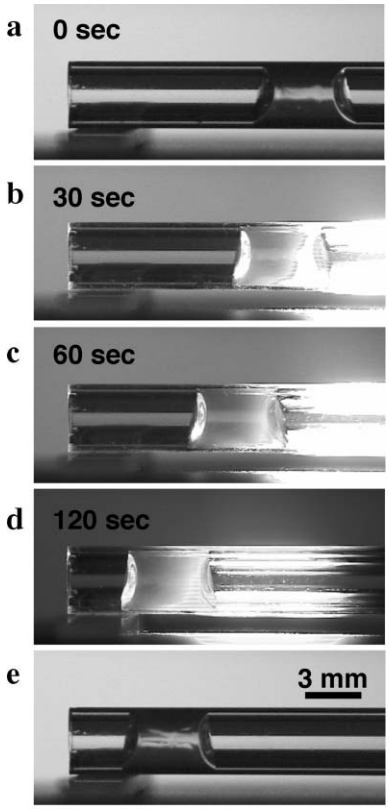

Fig. 7 Light-driven motion of an NPC-02 droplet within a capillary tube. The inside of the tube 2.3 mm in diameter was modified with H-CRA-CM in advance. (a) A droplet of NPC-02 was placed in the tube and exposed to UV light. (b, c and d) Subsequent irradiation with blue light at the right edge pushed the droplet to the left. (e) The droplet moved ~7 mm in 120 s.

droplet,[16,17,44]

$$F_h = \gamma_L(\cos\theta_e - \cos\theta) \quad (1)$$

where γ_L is the surface tension of the liquid. The dynamics of spreading of the droplet is controlled by conversion of capillary potential energy into viscous dissipation inside the droplet. The resulting spreading velocity is given by[44]

$$V = \frac{\theta\gamma_L(\cos\theta_e - \cos\theta)}{3\eta_L l} \quad (2)$$

where V is the spreading velocity, η_L is the viscosity of the liquid, and l is a logarithmic factor involving cut-off distances to the dissipative zone of the droplet.

Eqn. (2) shows that the spreading velocity is governed by the degree of change in the contact angle and both the viscosity and surface tension of the liquid. However, if the contact angle hysteresis of the liquid is not zero, the kinetics of spreading is modified significantly and depends on the bulk viscoelastic properties of the solid surface.[45] Thus a detailed calculation of the spreading speed of a liquid droplet on an H-CRA-CM-modified substrate requires knowledge of the dynamic properties of the solid surface.

Fig. 8 shows a schematic of the motion of a liquid droplet lying on a photochemically induced inhomogeneous surface. Suppose that γ_S^A, the surface tension of the solid at A (*cis*-rich surface), is larger than the value of γ_S^B at B (*trans*-rich surface). The net spreading tensions at A and B are given by[46]

$$\begin{aligned} t^A &= \gamma_S^A - \gamma_{SL}^A - \gamma_L^A\cos\theta_A(\text{to the left}) \text{ and} \\ t^B &= \gamma_S^B - \gamma_{SL}^B - \gamma_L^B\cos\theta_B(\text{to the right}) \end{aligned} \quad (3)$$

Accordingly the tension to the left is described by

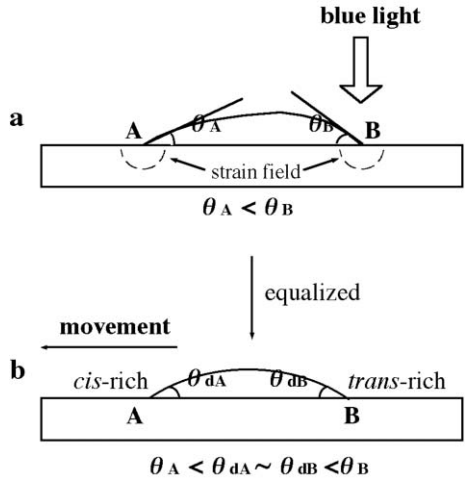

Fig. 8 Cross-section of a liquid droplet on a surface having a surface energy gradient. (a) The droplet may not move because the net spreading tension is zero (an idealized diagram). (b) The droplet moves in the direction of higher surface energy with a dynamic contact angle θ_d being smaller than θ_B and larger than θ_A.

$$\begin{aligned} t &= t^A - t^B = (\gamma_S^A - \gamma_S^B) - (\gamma_{SL}^A - \gamma_{SL}^B) - (\gamma_L^A\cos\theta_A - \gamma_L^B\cos\theta_B) \\ &= \Delta\gamma_S - \Delta\gamma_{SL} - (\gamma_L^A\cos\theta_A - \gamma_L^B\cos\theta_B) \end{aligned} \quad (4)$$

where θ_A and θ_B are not necessarily equilibrium contact angles. On the gradient surface, γ_L^A and γ_L^B may be equal, and because γ_{SL} is in general lower than γ_S, $\Delta\gamma_S$ would be larger than $\Delta\gamma_{SL}$. In this case, t is zero only if $\cos\theta_A > \cos\theta_B$ (Fig. 8(a)). Thus if the liquid droplet has asymmetrical contact angles that lead to t being zero, the droplet does not move. However, such a situation is ideal and cannot be obtained in actual cases. The asymmetrical drop shape causes a Laplace pressure gradient inside the droplet.[16] The pressure inside the droplet is rapidly equilibrated (t becomes greater than zero). Consequently, the Laplace pressure prevents the difference in the two contact angles from becoming large enough to reduce t to zero (Fig. 8(b)). This situation leads to uncompensated Young forces (imbalance in contact angles) and can lead to a directional motion of the droplet to the left with a dynamic contact angle between θ_A and θ_B.

Our experimental observations clearly support the driving mechanism stated above. Fig. 9 plots the time evolution of the directional motion of an NPC-02 droplet on a *cis*-rich surface by asymmetrical irradiation with blue light. As shown in Fig. 9, the advancing front of the droplet did not move at all for ~20 s in the early stages of irradiation, although the diameter of the droplet decreased. This dewetting phenomenon caused an increase in contact angles of both the advancing and receding edges of the droplet, because the pressure inside the droplet equilibrates rapidly.[16] The dewetting process continues until the droplet reaches a state in which the imbalanced Young's force is sufficient to move itself. After the initial induction period, the droplet started to move at a dynamic contact angle of ~20°,[47] which is an intermediate value between θ_{adv}^{cis} and θ_{rec}^{tr}. This leads to an imbalance in the contact angles; the advancing (~20°) and receding (~20°) edges of the moving droplet are on *cis*-rich (θ_{adv}^{cis} = 11°) and *trans*-rich (θ_{rec}^{tr} = 24°) surfaces, respectively.

Liquid motion driven by changes in interfacial temperature

Surface tension generally decreases with increasing temperature because thermal motion disrupts the intermolecular interactions and tends to make the environment of the molecules in the bulk similar to those at the surface.[11] A contact angle in equilibrium, however, is a function of three

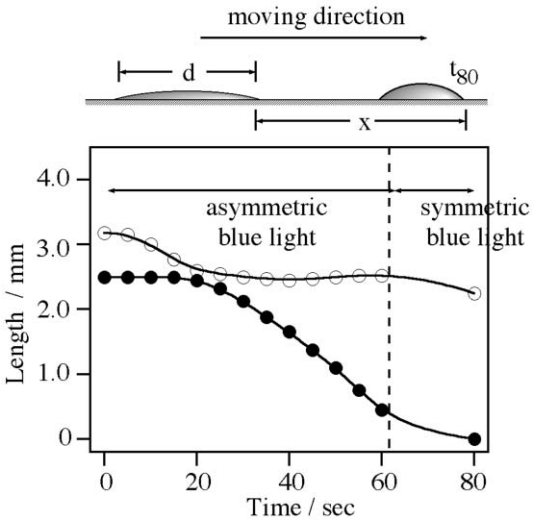

Fig. 9 Changes in position (x, closed circles) and diameter (d, open circles) of the moving NPC-02 droplet on an H-CRA-CM-modified plate as a function of time. Photoirradiation of the plate was carried out by the same procedure as shown in Fig. 3. A speed of 50 μm s^{-1} was observed for the motion of ~2 μl droplet.

parameters as described by the Young equation. The equation indicates that wetting is favored by low interfacial free energy and high solid surface free energy as well as low liquid surface free energy. Generally the temperature effect on contact angles is not very large.[48] On the other hand, a sudden transition of a liquid such as the nematic/isotropic phase transition of LCs should give rise to distinctive changes in contact angle as a function of temperature. Indeed, Gannon and Faber found a valuable phenomenon with nematic LCs; ($d\gamma/dT$) is positive in sign both for the isotropic phase just above T_{NI} and for the nematic phase just below it.[49] The authors explained the results assuming that there is an excess level of molecular order at the surface layers, *i.e.* the surface of the liquid forms a smectic-like structure even when the bulk is nematic or isotropic.

Fig. 10 shows the contact angles as a function of temperature for 1-bromonaphthalene and NPC-02 (T_{NI} = 35.0 °C) on an H-CRA-CM-modified substrate. 1-Bromonaphthalene (mp = −2 °C, bp = 279–281 °C) was chosen for comparison

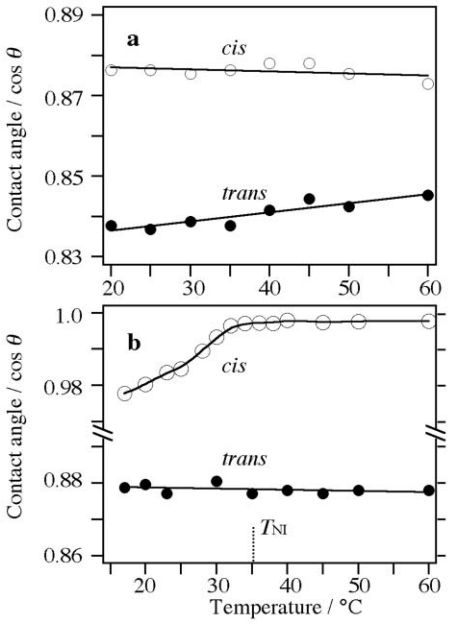

Fig. 10 Temperature dependence of contact angles for 1-bromonaphthalene (a) and NPC-02 (b) on H-CRA-CM monolayers before (filled) and after (open) irradiation with UV light.

with the nematic LC, NPC-02. The contact angles of 1-bromonaphthalene on both the *trans*- and *cis*-H-CRA-CM monolayers are insensitive to temperature within the limit of experimental error when the temperature was raised from 20 °C to 60 °C (Fig. 10(a)). The value of ($d\gamma/dT$) for the *trans*-H-CRA-CM monolayer was −0.02, which is similar to the value of common liquids on a solid substrate.[11] A similar trend in the contact angle changes of NPC-02 on the *trans*-H-CRA-CM monolayer was observed (Fig. 10(b)). Any discontinuity due to the phase transition of NPC-02 was not observed. In contrast, contact angles on the *cis*-H-CRA-CM monolayer significantly decreased when the sample temperature was raised from 15 °C to 35 °C, followed by leveling off above 35 °C. The reason for this feature is not fully understood. However, because the contact angle values obtained for the *trans*-H-CRA-CM monolayer are not altered in the same temperature range, it is unlikely that the decrease in contact angles on the *cis*-H-CRA-CM monolayer can be attributed to a decrease in γ_L or the nematic/isotropic phase transition of NPC-02. We believe that the phenomenon is caused by a decrease in the surface free energy of the LC/monolayer interface, suggesting a higher affinity between LC and surface molecules at a higher temperature.

A temperature gradient of a solid surface can cause liquids on the surface to move.[18–20] Results showing that contact angles of NPC-02 on the *cis*-H-CRA-CM monolayer are significantly modified by temperature changes (Fig. 10(b)) lead us to examine *in situ* and reversible motions of an NPC droplet based on changes in temperature. As shown in Fig. 11(a), the spreading/retraction motion can be driven by changes in the surface temperature. Thus, if one creates a spatial temperature gradient in the area of a liquid droplet, the droplet should move in the direction of the higher temperature. Fig. 5–11(b) demonstrates that the reversible change in sessile contact angles upon alternating irradiation with UV and blue light at 40 °C is as large as 22° .

Applications to on-chip chemical reactions

Light-driven liquid motion provides an alternative pumping method that is simple, inexpensive and efficient for small capillary systems, as demonstrated in Fig. 7. Compared to the conventional electroosmotic method, one of the major advantages of the light-driven method stems from a lack of necessity of an electrolyte dissolved in a fluid. This suggests that the photochemical method is applicable to operate on-chip organic synthesis by illumination. Fig. 12 shows a fluorescence labeling reaction of fluorescamine and dodecylamine dissolved separately in two NPC-02 droplets placed on an H-CRA-CM-modified silica plate. The reaction was chosen because it is very fast and generates a fluorescent product, which is easily detected by UV light irradiation. An NPC-02 droplet

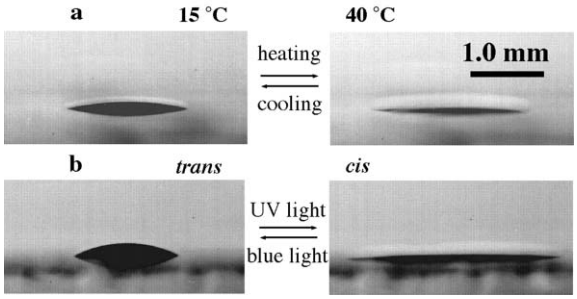

Fig. 11 (a) Lateral photographs of *in situ* spreading/retraction motion of an NPC-02 droplet on an H-CRA-CM-modified plate driven by temperature changes between 15 °C and 40 °C. The sessile contact angles are 12° and 4°, respectively. (b) The spreading/retraction motion upon alternating irradiation with UV and blue light at 40 °C. The sessile contact angles are 26° and 4°, respectively.

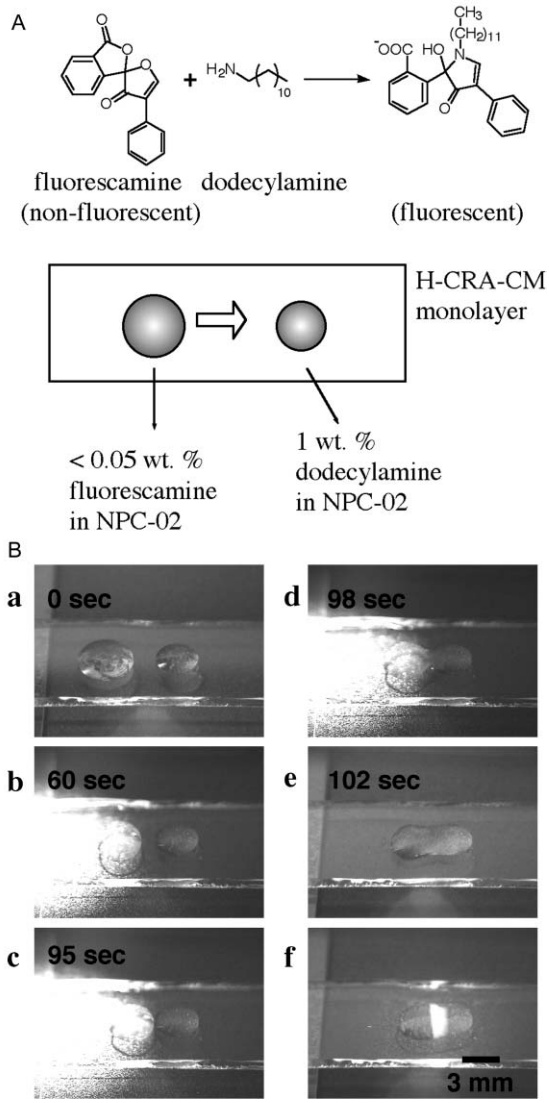

Fig. 12 A fluorescence labeling reaction operated by light on an H-CRA-CM-modified plate. The delivery of an NPC-02 droplet containing the fluorescence reactant (<0.05 wt% fluorescamine) is performed by asymmetric illumination of the droplet with blue light. The illumination causes the NPC-02 droplet to move continuously (a, b and c) and finally to contact with an NPC-02 droplet containing 1 wt% dodecylamine (d and e). The product formed is detected by irradiation with UV light (f).

containing the fluorescence reagent was asymmetrically illuminated so that it moved towards an NPC-02 droplet containing dodecylamine (Fig. 12 (b) and (c)). Both droplets finally coalesced (Fig. 12 (d) and (e)). Irradiation of the mixed fluid with UV light allows detection of the reaction product, which fluoresces strongly (Fig. 12(f)).

Conclusions

The present work demonstrates the use of light to move liquids on a photoresponsive monolayer, thereby providing new principles for the operation of micro-scale chemical process systems. The light-driven motion of liquids was achieved by an appropriate choice of photoresponsive molecules tethered to a solid surface and fluid substances. The motion of liquid droplets was examined by placing them on an H-CRA-CM-modified substrate, followed by photoirradiation with UV and blue light to trigger the isomerization of the azobenzene moieties assembled on the surface. Gradients in surface free energy were created by asymmetrical illumination of the surface. The resulting spatially controlled changes in the photoisomerization of surface-immobilized azobenzenes allowed the directional motion of the droplet. Contact angle measurements for various liquids revealed that hysteresis effects are critical to realize liquid motion. The direction of liquid motion was tailored by manipulating the direction of the gradient of light intensity. Detailed profiles for the moving droplet support the hypothesis that the light-driven motion is ascribed to an imbalance in contact angles. The potential applicability of light-driven liquid motion was demonstrated by the delivery of reactants for a chemical reaction on a photoresponsive surface.

Performance improvements in light-operated fluidic systems on the basis of the present method may require a photochromic molecular system that shows larger changes in surface free energy upon illumination. This approach will enable us to achieve rapid manipulation of the motion of liquids, including aqueous solutions and to find applications in a broad range of areas from on-chip synthesis to microfluidic devices.

Acknowledgement

This work was supported by a Grant for "Harmonized Molecular Materials" from NEDO (New Energy Development Organization).

References

1 B. H. Weigl and P. Yager, *Science*, 1999, **283**, 346.
2 K. Petersen, *Sens. Actuators. A*, 1996, **74**, 143.
3 M. U. Kopp, A. J. de Mello and A. Manz, *Science*, 1998, **280**, 1046.
4 M. A. Burns, B. N. Johnson, S. N. Brahmasandra, K. Handique, J. R. Webster, M. Krishnan, T. S. Sammarco, P. M. Man, D. Jones, D. Heldsinger, C. H. Mastrangelo and D. T. Burke, *Science*, 1998, **282**, 484.
5 J. T. Santini, M. J. Cima and R. Langer, *Nature*, 1999, **397**, 335.
6 R. D. Chambers and R. C. H. Spink, *Chem. Commun.*, 1999, 883.
7 D. J. Harrison, K. Fluri, K. Seiler, Z. Fan, C. S. Effenhauser and A. Manz, *Science*, 1993, **261**, 895.
8 H. Salimi-Moosavi, T. Tang and D. J. Harrison, *J. Am. Chem. Soc.*, 1997, **119**, 8716.
9 F. von Heeren, E. Verpoorte, A. Manz and W. Thormann, *Anal. Chem.*, 1996, **68**, 2044.
10 D. C. Duffy, J. C. McDonald, O. J. A. Schueller and G. M. Whitesides, *Anal. Chem.*, 1998, **70**, 4974.
11 A. W. Adamson and A. P. Gast, *Physical Chemistry of Surfaces*, 6th edn., John Wiley & Sons, New York, 1997.
12 L. Leger and J. K. Joanny, *Rep. Prog. Phys.*, 1992, 431.
13 L. H. Tanner, *J. Phys. D: Appl. Phys.*, 1979, **12**, 1473.
14 R. G. Cox, *J. Fluid Mech.*, 1986, **168**, 418.
15 T. Ondarcuhu and M. Veyssié, *Nature*, 1991, **352**, 1539.
16 F. Brochard, *Langmuir*, 1989, **5**, 432.
17 M. K. Chaudhury and G. M. Whitesides, *Science*, 1992, **256**, 1539.
18 N. O. Young, J. S. Goldstein and M. J. Block, *J. Fluid Mech.*, 1959, **6**, 350.
19 K. D. Barton and R. S. Subramanian, *J. Colloid Interface Sci.*, 1989, **133**, 211.
20 A. M. Cazabat, F. Heslot, S. M. Troian and P. Carles, *Nature*, 1990, **346**, 824.
21 L. E. Scriven and C. V. Sternling, *Nature*, 1960, **187**, 186.
22 P. Carles and A. M. Cazabat, *Colloids Surf.*, 1989, **41**, 97.
23 A. F. M. Leenaars, J. A. M. Huethorst and J. J. van Oekel, *Langmuir*, 1990, **6**, 1701.
24 B. S. Gallardo, V. K. Gupta, F. D. Eagerton, L. I. Jong, V. S. Craig, R. R. Shah and N. L. Abbott, *Science*, 1999, **283**, 57.
25 D. E. Bennett, B. S. Gallardo and N. L. Abbott, *J. Am. Chem. Soc.*, 1996, **118**, 6499.
26 S.-K. Lee and P. E. Laibinis, *J. Am. Chem. Soc.*, 2000, **122**, 5395.
27 (*a*) C. D. Bain and G. M. Whitesides, *J. Am. Chem. Soc.*, 1988, **110**, 5897; (*b*) G. M. Whitesides and P. E. Laibinis, *Langmuir*, 1990, **6**, 87.
28 (*a*) K. Aoki, Y. Kawanishi, T. Seki, M. Sakuragi, T. Tamaki and K. Ichimura, *Liq. Cryst.*, 1995, **19**, 119; (*b*) L. M. Siewierski, W. J. Brittain, S. Petrash and M. D. Foster, *Langmuir*, 1996, **12**, 5838; (*c*) G. Möller, M. Harke and H. Motschmann, *Langmuir*, 1998, **14**, 4955.

29 (*a*) M. O. Wolf and M. A. Fox, *J. Am. Chem. Soc.*, 1995, **117**, 1845; (*b*) M. O. Wolf and M. A. Fox, *Langmuir*, 1996, **12**, 955; (*c*) M. A. Fox and M. D. Wooten, *Langmuir*, 1997, **13**, 7099; (*d*) S. Abbott, J. Ralston, G. Reynolds and R. Hayes, *Langmuir*, 1999, **15**, 8923.
30 K. Ichimura, *Chem. Rev.*, 2000, **100**, 1847.
31 M. Ueda, H.-B. Kim and K. Ichimura, *J. Mater. Chem.*, 1994, **4**, 883.
32 (*a*) I. Willner and S. Rubin, *Angew. Chem., Int. Ed. Engl.*, 1996, **35**, 367; (*b*) I. Willner and R. Blonder, *Thin Solid Films*, 1995, **266**, 254.
33 *Photochromism: Molecules and Systems*, ed. H. Dürr and H. Bouas-Laurent, Elsevier, Amsterdam, 1990.
34 K. Ichimura, S.-K. Oh and M. Nakagawa, *Science*, 2000, **288**, 1624.
35 K. Ichimura, S.-K. Oh, M. Fujimaki, Y. Matsuzawa and M. Nakagawa, *J. Inclusion Phenom. Macrocyclic Chem.*, 1999, **35**, 173.
36 S.-K. Oh, M. Nakagawa and K. Ichimura, *Chem. Lett.*, 1999, 349.
37 (*a*) M. Fujimaki, S. Kawahara, Y. Matsuzawa, E. Kurita, Y. Hayashi and K. Ichimura, *Langmuir*, 1998, **14**, 4495; (*b*) K. Ichimura, N. Fukushima, M. Fujimaki, S. Kawahara, Y. Matsuzawa, Y. Hayashi and K. Kudo, *Langmuir*, 1997, **13**, 6780.
38 N. Tillman, A. Ulman, J. S. Schildkraut and T. L. Penner, *J. Am. Chem. Soc.*, 1998, **110**, 6136.
39 M. K. Chaudhury, *Mater. Sci. Eng.*, 1996, **R16**, 97.
40 (*a*) Y. L. Chen, C. A. Helm and J. N. Israelachvili, *J. Phys. Chem.*, 1991, **95**, 10736; (*b*) H. Yoshizawa, Y.-L. Chen and J. Israelachvili, *J. Phys. Chem.*, 1993, **97**, 4128.
41 (*a*) W. Chen, A. Y. Fadeev, M. C. Hsieh, D. Öner, J. Youngblood and T. J. McCarthy, *Langmuir*, 1999, **15**, 3395; (*b*) A. Y. Fadeev and T. J. McCarthy, *Langmuir*, 1999, **15**, 3759.
42 (*a*) W. Jin, J. Koplik and J. R. Banavar, *Phys. Rev. Lett.*, 1997, **78**, 1520; (*b*) L. W. Schwartz and S. J. Garoff, *Colloid Interface Sci.*, 1985, **106**, 422; (*c*) A. M. Schwartz, *J. Colloid Interface Sci.*, 1980, **75**, 404.
43 P. G. de Gennes, *Rev. Mod. Phys.*, 1985, **57**, 827.
44 D. Long, A. Ajdari and L. Leibler, *Langmuir*, 1996, **12**, 5221.
45 L. W. Schwartz, *Langmuir*, 1999, **14**, 3440.
46 S. B. Carter, *Nature*, 1967, **213**, 256.
47 The dynamic contact angle was retained during the motion, and the difference between the advancing and receding dynamic contact angles was less than 2°.
48 (*a*) M. C. Phillips and A. C. Riddiford, *Nature*, 1965, **205**, 1005; (*b*) H. Schonhorn, *Nature*, 1966, **210**, 896; (*c*) J. B. Jones and A. W. Adamson, *J. Phys. Chem.*, 1968, **72**, 646.
49 M. G. J. Gannon and T. E. Faber, *Phil. Mag.*, 1978, **37**, 117.